DESIGN AND SENSITIVITY ANALYSIS OF AXIAL-FLUX PERMANENT MAGNET SYNCHRONOUS MACHINE

[1]Mostafa. AHMADI DARMANI **[2]Hooman. HOOSHYAR**
[1]Faculty of Electrical and Computer Engineering, Science and Research Branch, Islamic Azad University, Tehran, Iran, Phone: +989121382532, Email: mostafa.ahmadi.d@gmail.com
[1]Faculty of Electrical and Computer Engineering, Science and Research Branch, Islamic Azad University, Tehran, Iran, Phone: +989126131968, Email: hoomanhooshyar@gmail.com

Abstract *– Design aspects of the Axial Flux Permanent Magnet (AFPM) machines are discussed in this paper. Also a particular attention is given on design and performance analysis of AFPM machine to study influence of initial design parameters, air-gap flux density, electrical loading, current density, diameter ratio on machine efficiency. A comprehensive approach is used for design of AFPM machine. Then design flowchart of AFPM machines is presented. Optimal design of axial flux permanent magnet machine with the purpose of enhancing machine efficiency is found by using genetic algorithm. A 3-phase, 11 kW, double-stage AFPM synchronous machine with two stators and rotor is designed and then three dimensional finite element analyses is performed to validate the design procedure. It is found that the results completely agree with the presented procedure. Furthermore, the influence of slot opening is investigated on performance of AFPM machines.*

Keywords*: Axial Flux Permanent Magnet (AFPM) Machine, Sizing Equations, Genetic Algorithm (GA), Analytical Method, Sensitivity Analysis, Finite Element Analysis (FEA), Slot Opening*

1. Introduction

The development in the manufacturing of permanent magnets makes them available in different grades, which include a wide range of properties and application requirements. Thus, electrical machines account remarkable value of total global electricity consumption [1-2].

The electrical machines which are using permanent magnet (PM) in their construction have become more attractive option than other kinds. PM machines have more efficiency, higher power and/or torque density, better dynamic performance, simple construction and maintenance.

Among the PM electrical machines, Axial Flux Permanent Magnet (AFPM) machines topology provides a higher power-to-weight ratio that it causes smaller core and higher efficiency [3-6]. This advantage makes AFPM machines appropriate candidate for electrical vehicles and aircrafts [7]. Furthermore, according to their extreme axial compactness and thin structure, they are proper for using in pumps, fans and household applications [8-10]. AFPM machines are also used in generation system as generator of wind turbines [11] and micro turbines [12-13].

In this paper, the entire equations required for AFPM machine design are presented in Section II and III. Moreover, overall design concerns and restrictions for an AFPM machine are presented in Section II. Some features of GA and an objective function with the aim of high efficiency subjected to practical and performance restrictions are introduced in Section IV. In Section V, sensitivity analysis is used to reach design domination and recognize machine behavior on design criteria. In Section VI, a computer aid program for design of an AFPM machine using GA is attempted. In Section VII the details of the design procedure are given and then the design validation is proved by three dimensional finite element analysis. The effect of slot opening on machine performance is studied in Section VIII. Finally, conclusions are given in Section IX.

2. Sizing Procedure

The design procedure of a rotating electrical machine is shown in Fig.1.

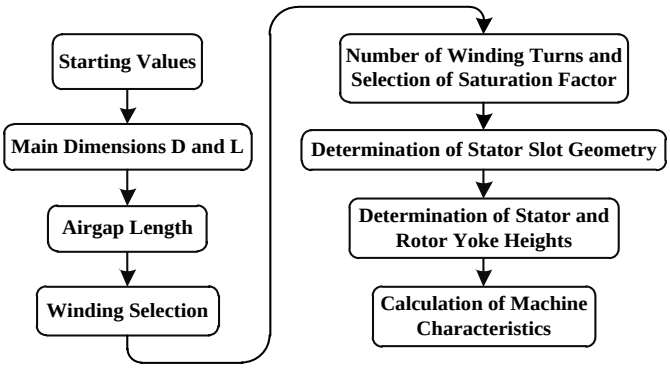

Fig. 1. Design procedure of a rotating electrical machine

The design of a PM electrical machine can be commenced by defining certain basic characteristics such as output power, rated speed or rated angular speed, rated frequency, rated voltage, number of phases, and number of pole pairs and slots of the machine [14].

The criteria for choosing promising slot/pole

combinations (Ns/2p) have been presented by several authors and can be summarized as follows [15-17]:

The winding factor should be high to produce high torque.

The lowest common multiple (LCM) between the number of poles and slots should be high.

The greatest common divisor (GCD) between the number of poles and slots should be high and also an even number.

2.1 PM Air-gap Flux Density

In permanent magnet machines, the air-gap flux density must be in a sensible relation to the remanent flux density of the permanent magnet material. From the economy point of view of this material, the maximum air-gap flux density with permanent magnets should be about half of the remanent flux density.

The required thickness of the PM "h_{PM}" to obtain desired air-gap flux density is calculated as [3]:

$$h_{PM} = \frac{\mu_{r,PM} B_g k_{Carter} g}{0.95 B_r - \frac{B_g}{\sigma_{L,PM}}} \quad (1)$$

Where "$\mu_{r,PM}$" is permanent magnet relative permeability, "B_g" air-gap flux density, "k_{Carter}" Carter coefficient, "g" axial length of air-gap, "$\sigma_{L,PM}$" is leakage factor which is used to model the wasting flux density. In [18] and [19] the leakage factor is calculated by analytical method for PM machines.

2.2 Winding Selection

Choosing an appropriate winding for machine is very important. This is a critical phase with respect to the final characteristics of the machine. A guiding attitude is that a polyphase winding with high slot number produces more sinusoidal current linkage.

Different kind of winding is used in AFPMs. Distributed winding, concentrated winding and drum winding are three most common used windings. Among the mentioned windings, concentrated winding is mostly used in AFPMs because of low end winding, low copper cost owing to less coils, simple winding structure, and simple stator core for different number of phases [5]-[20].

2.3 Main Sizing Equations

For each electric machine, if stator leakage inductance and resistance are neglected, the electromagnetic apparent power is defined as:

$$S_{Elm} = \epsilon \frac{P_{out}}{\eta \cos(\varphi)} \quad (2)$$

where "P_{out}" is output power, "η" is machine efficiency, "$cos(\varphi)$" is power factor and the coefficient "ϵ" is the ratio of the EMF induced by the rotor excitation flux at no-load "E_f" to the machine terminal voltage "V_{ph}" and defined by equation (3):

$$\epsilon = \frac{E_f}{V_{ph}} = \begin{cases} Motor, & \epsilon < 1 \\ Generator, & \epsilon > 1 \end{cases} \quad (3)$$

Note that in permanent magnet machines E_f is $e_{ph,PM}$. Also the output power of machine can be expressed as:

$$P_{out} = \eta m \frac{1}{T} \int_0^T e_{ph,PM}(t) i_s(t) dt = \eta m K_p e_{ph,PM} i_s \quad (4)$$

where "$e_{ph,PM}(t)$" is the phase EMF induced by the PM, "$e_{ph,PM}$" is the peak value of EMF, "$i_s(t)$" is the phase current, "i_s" is the peak value of phase current and "m" is number of stator phase. The quantity "K_P" is termed the electrical power waveform factor and it is defined as:

$$K_p = \frac{1}{T} \int_0^T \frac{e(t) \times i(t)}{e_{ph,PM} \times i_s} dt = \frac{1}{T} \int_0^T f_e(t) f_i(t)\, dt \quad (5)$$

For AFPM machines, the peak value of the phase air-gap EMF and the peak value of the phase current can be expressed as:

$$e_{ph,PM} = K_e N_{ph} B_g \frac{\omega}{p} (1 - k_d^2) D_{out}^2 \quad (6)$$

$$i_s = \frac{\pi K_i A (1 + k_d) D_{out}}{2 m N_{ph}} \quad (7)$$

"K_e" is the EMF factor which incorporates winding distribution factor "K_w" and per-unit portion of air-gap area-total spanned by the machine's salient poles (if any) [21]. Also, "N_{ph}" is number of coil turns in series per phase winding. For a surface-mounted AFPM machine the coefficient "k_e" is equal to the value [14].

$$K_e = \frac{\pi}{8} \frac{W_{PM}}{\tau_{pole}} \quad (8)$$

"W_{PM}" is magnet width and "τ_{pole}" is pole pitch.

In AFPM machines, the diameter ratio "k_d" is an important design parameter which has significant effect on the characteristics of the machine. To operate the machine in optimized state, the value of k_d has to be chosen carefully. The torque production capability of AFPM machines, as a function of k_d, is described in Fig. 2. The curve is scaled for the maximum torque to be equal to value 1. The optimum value of k_d is equal to

$\frac{1}{\sqrt{3}} = 0.57735.$

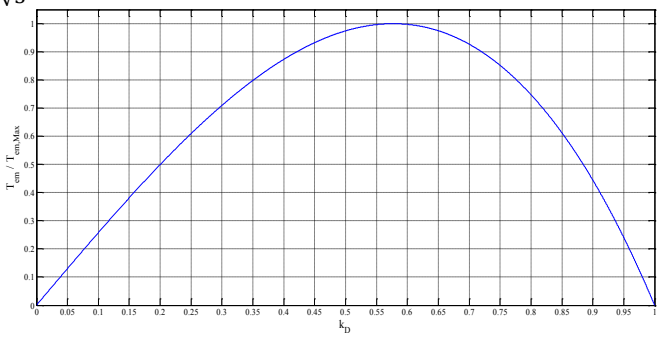

Fig. 2. Torque as a function of k_d

Substitution of (6) and (7) into (4) yield an expression for the output power of an AFPM machine:

$$P_{out} = \frac{\pi}{2}\eta K_p K_e K_i B_g A \frac{\omega}{p}(1-k_d^2)(1+k_d)D_{out}^3 \quad (10)$$

where "*A*" is electrical loading, "p" is number of pole pairs, "ω" is angular frequency and "D_{out}" is outer diameter.

The outer diameter of the stator is the most important dimension of AFPM motors and it can be expressed as:

$$D_{out} = \sqrt[3]{\frac{\epsilon P_{out}}{\frac{\pi}{2}\eta K_p K_e K_i B_g A \frac{\omega}{p}(1-k_d^2)^2(1+k_d)}} \quad (11)$$

The external diameter of the AFPM machine can be calculated by:

$$D_{ext} = D_{out} + 2l_{end} \quad (12)$$

where "l_{end}" is radial length of the end-winding and it can be calculated by:

$$l_{end} = l_e + 3\sqrt{\frac{S_{Cu}}{\pi k_{Cu}}} \quad (13)$$

where "l_e" is the constant describing the distance between the stator core, "k_{Cu}" copper fill factor and end-winding and "S_{Cu}" is the cross sectional area of copper per phase and pole [22].

2.1 Rotor Core Geometry

The thickness of the stator yoke can be calculated as [3]:

$$L_{yr} = \frac{B_g \pi D_{out}(1+k_d)}{B_{cr} 8p} \quad (14)$$

$$B_{cr} = \begin{cases} 5.47 f^{-0.32}, & f > 40 \\ 1.7 \quad to \quad 1.8, & f \le 40 \end{cases} \quad (15)$$

Calculating the maximum deflection value of rotor is very important. For an AFPM machine, deflection can be calculated by [23]:

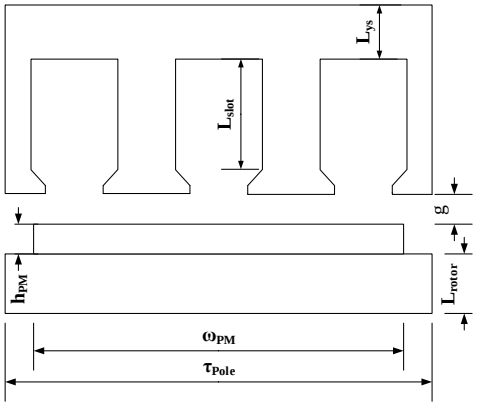

Fig. 3. Main dimension of machine

$$Y_{Deflection} = M\frac{r_{out}^2}{D}K + Q_N\frac{r_{out}^3}{D}K' - q\frac{r_{out}^4}{D}K'' \quad (16)$$

$$q = \frac{B_g^2}{2\mu_0} \quad (17)$$

$$Q_N = \frac{q}{2r_{shaft}}(r_{out}^2 - r_{in}^2) \quad (18)$$

where "*M*" is radial bending moment of shaft, "Q_N" is shear force, "D" plate constant, "r_{shaft}" is shaft radius, "*K*, *K'*, *K''*" are constants depending on inner and outer diameters of machine. Also "*q*" is Maxwell stress.

2.2 Stator Core Geometry

The thickness of the stator yoke can be calculated based on the air-gap flux and the allowed flux density in the stator yoke as [3]:

$$L_{ys} = \frac{B_g \pi \alpha_p D_{out}(1+k_d)}{8pB_{ys}} \quad (19)$$

$$B_{ys} = 4.38 f^{-0.32} \quad (20)$$

The required stator yoke thickness is depending on the machine magnetic loading and mechanical characteristics. If the number of pole pairs is small, stator yoke thickness will be determined by machine specific loading. As it is shown in figure 4, if the number of pole pairs were large, the stator yoke thickness will be very thin, therefore mechanical constructions is determining the stator yoke thickness. In this situation, the stator yoke thickness is dependent to natural frequency of stator, height of the stator teeth and winding.

Natural frequency of stator yoke "f_{ns}" is expressed by Young method [24]:

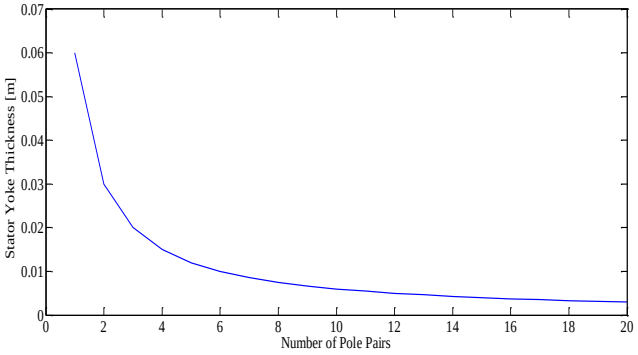

Fig. 4. Stator yoke thickness as function of pole pairs

$$f_{ns} = \frac{1}{2\pi}\sqrt{\frac{K_{fn}}{M_{fn}}} \tag{21}$$

where "K_{fn}" is the lumped stiffness and "M_{fn}" is the lumped mass.

2.3 Carte's Coefficient

To be able to calculate the magnetic voltage manually over the air-gap, the geometry of the air-gap has to be simplified. Often in an electrical machine, the surfaces of both the stator and the rotor are split with slots. The flux density always decreases at the slot opening and therefore it is not easy to define the average flux density of the slot pitch between the stator and the rotor.

$$g_e = gk_{Carter} \tag{22}$$

The equivalent slot opening in which the flux density is zero, is:

$$b_e = k_{Carter}b \tag{23}$$

The Carter factor is:

$$k_{Carter} = \frac{\tau_{Slot,ave}}{\tau_{Slot,ave} - \gamma g} \tag{24}$$

$$\gamma = \frac{4}{\pi}\left[\frac{b}{2g}tg^{-1}\left(\frac{b}{2g}\right) - Log\sqrt{1+\left(\frac{b}{2g}\right)^2}\right] \approx \frac{b}{5g+b} \tag{25}$$

The Carter factor is also the ratio of the maximum flux density B_{Max} to the average flux density B_{ave}:

$$k_{Carter} = \frac{B_{Max}}{B_{ave}} \tag{26}$$

2.4 Stator Slot Geometry

A semi-closed slot is shown in Fig. 5. Because of disk structure of stator in AFPMs, by incrementing machine diameter from in to out, the slot teeth width increases. The slot teeth width in inner diameter has the minimum value, so the minimum geometry of sot is determined. Therefore, the minimum required dimensions of the slot are determined based on teeth width in inner diameter. Moreover, saturation of slot teeth is one of the important factors to determine slot geometry.

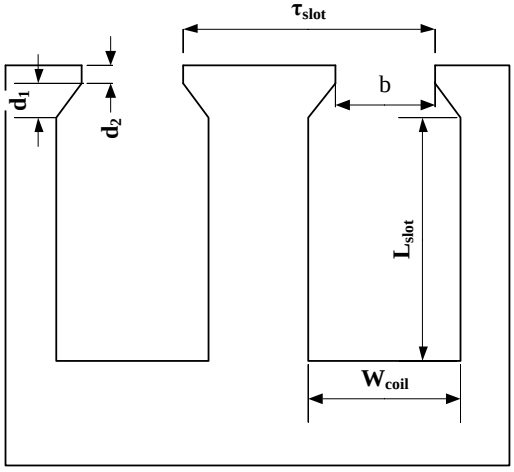

Fig. 5. Geometry of stator slot

Cross section of each conductor is:

$$S_a = \frac{I_{ph}}{a_p J_s} \tag{27}$$

Current density "J_s" is determined by cooling system. Number of coil conductors in one slot is:

$$N_{Coil} = \frac{a_p N_{ph}}{Q/_m} \tag{28}$$

Cross section of slot "S_{Slot}" should be applied in the following conditions [25]:

$$S_{Slot} \geq \frac{S_a}{k_{Cu}} \tag{29}$$

The minimum cross section of copper for each slot "S_{Cu}" is:

$$S_{cu} = \frac{2S_a N_{Coil}}{k_{cu}} \tag{30}$$

The coil span is:

$$W_{Slot} = \tau_{Slot,min} - C_{min} \tag{31}$$

Where "C_{min}" is tooth width in inner diameter. The minimum value of tooth width in inner diameter should be determined based on maximum flux density and mechanical constrains.

Now the slot length is:

$$l_{Slot} = \frac{W_{Coil}}{S_{cu}} \tag{32}$$

3. Losses and Efficiency Calculation

3.1 Phase Resistance and Copper Loss

Copper loss is one of the main losses of electrical machines. So, to estimate accurate value of copper losses, it is important to find the phase resistance of the machine. Resistance of copper wires is depending on the temperature. Also it will be essential to determine the temperature of windings. The phase resistance is defined as [12]:

$$R_{ph} = \frac{l_{Cu}\left(1 + K_{T,Cu}(T-20)\right)}{\sigma_{Cu} S_{Cu} a_p} \quad (33)$$

where "l_{Cu}" is the length of winding, "$K_{T,Cu}$" is temperature coefficient of copper, "T" is coil temperature, "σ_{Cu}" is electric conductivity of copper and "α_p" is number of parallel paths or conductors.

The length of winding is determined by [12]:

$$l_{Cu} = 2N_{ph}\big(l_s + (0.083p + 1.217)\tau_{pole,ave} + 0.02m\big) \quad (34)$$

Where "l_s" and "$\tau_{pole,ave}$" are the length of the stator stack and pole pitch in average radius respectively.

The copper loss can be calculated by:

$$P_{Cu} = m R_{ph} {I_{ph}}^2 \quad (35)$$

The stator`s high frequency current and high frequency magnetic field cause eddy current losses and it is defined as [26]:

$$P_{eddy,Cu} = \frac{V_{Cu}\left(2\pi f B_g d_w\right)^2}{32\rho_{Cu}} \times 10^{-3} \quad (36)$$

where "V_{Cu}", "d_w", and "ρ_{Cu}" are copper volume, diameter of each wire of conductor and resistivity of copper, respectively.

3.2 Core Losses

Due to the complicated phenomena in laminated core, calculating core losses is too difficult. Up to now, deferent methods are presented. The best way to calculate core loss is to classify it into three parts, hysteresis losses, eddy current losses, and excess losses.

According to the classification, the core losses per unit volume can be expressed:

$$P_{Fe} = k_{hys}\hat{B}^2 f + \pi^2 \frac{\sigma_{Fe} d^2}{6}\left(\hat{B}f\right)^2 + 8.67.k_{exc}\left(\hat{B}f\right)^2 \quad (37)$$

where "k_{hys}" Coefficient of hysteresis losses and "k_{exc}" excess losses are obtained based on core losses of the machine in deferent frequencies. Usually this information is presented by manufacturers.

Additional core losses which cannot be calculated easily are appeared as stray losses. The stray losses are consisted of two parts, harmonic losses in the ferromagnetic core of AC machines and other anomalous losses [12], [22].

$$P_{stray} = k_{stray} P_{output} \quad (38)$$

The coefficient "k_{stray}" is depending on the machine`s output power.

3.3 Eddy Current Losses in PMs and Rotor Disks

The main part of losses in permanent magnet machines and low-speed machines are copper and core losses. In addition, eddy current losses in PMs are appeared because of existence of harmonic component in air-gap flux density distortion. The eddy current losses are occurred in the permanent magnets and rotor disks. Usually the eddy current losses are neglected. But note that it is the main losses in high-speed machines. Also for semi-closed stator slot, the eddy current losses are not significant.

In this study we studied low-speed machine and used semi-closed slot. So calculation of eddy current was neglected. But using finite element method to calculation eddy current is suggested for open slot.

3.4 Mechanical Losses

Mechanical losses or rotational losses consist of mainly friction losses in bearings, winding losses and ventilation losses. Bearing losses is dependent on some factors such as, the bearing type, bearing diameter, rotor speed, load and lubricant used. Winding losses occur when friction is created with the rotating parts of the machine and the surrounding air. Unlike frictional loss, winding loss increases non-linearly with the speed. There are many semi-empirical equations for calculating the rotational losses giving various degrees of accuracy [13], [27].

$$P_{mech} = \frac{1}{2} c_f \rho_{air} (2\pi n)^3 \left(R_{out}^5 - R_{shaft}^5\right) \quad (39)$$

where "c_f" drag coefficient for turbulent flow and it can be found as:

$$c_f = \frac{3.87}{\sqrt{Re}} \quad (40)$$

That "Re" the Reynolds number for a rotating disk where its outer radius is:

$$Re = \frac{2\pi N_s \rho_{air} R_{out}^2}{\mu_{air}} \quad (41)$$

where "μ_{air}" is the dynamic viscosity of air.

3.5 Total Losses and Efficiency

Finally, total losses of the machine and the efficiency can be calculated by:

$$P_{Loss,total} = \sum P_{Loss} = P_{cu} + P_{stray} + P_{Fe} + P_{mech} \quad (42)$$

$$\eta = \frac{P_{out}}{P_{in}} = \frac{P_{out}}{P_{out} + \sum P_{Loss}} \quad (43)$$

In Fig 6 design procedure of axial flux PM machine is presented based on expressed sizing equations.

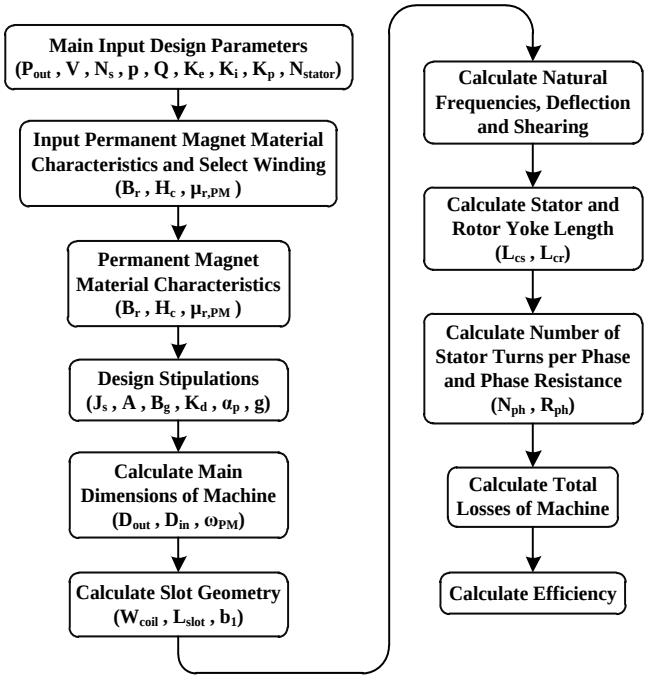

Fig. 6. Design procedure of AFPM Machine

4. Optimized Design of AFPM Machine

4.1 Fitness Function

Fitness function is based on minimizing the machine`s losses (copper losses, core losses, stray losses and mechanical losses) to reach maximum efficiency. By reducing copper losses, phase resistance will be decreased and by reducing core losses, the machine`s total volume will decrease too. Limitations of optimizing the function parameters are presented in table 1. Also lower and higher band of parameters are presented.

$$f_{opt}(B_g, A, J_s, k_d, \alpha_p, g) \quad (44)$$

Table 1. Fitness Function Variables

Variable	Sign	x_{min}	x_{max}
B_g	X_1	0.3	0.75
A	X_2	30 [kA/m]	75 [kA/m]
J_s	X_3	3[A/mm^2]	7.5[A/mm^2]
k_d	X_4	0.55	0.75
α_p	X_5	0.65	0.75
g	X_6	0.001 [m]	0.003 [m]

In low speed axial flux PM machines, copper losses are dominated and other losses are neglected. But in this study, we consider P_{Fe} and also we assumed that the P_{stray} is constant 1% of the output power to reach to the good accuracy. The mechanical losses and eddy current losses are neglected because the value of these losses is not significant.

4.2 Genetic Algorithms and Optimization

The Genetic Algorithms is an arbitrary universal research method that imitates the metaphor of a natural biological progress. GAs is capable for complicated optimization process by exploring an enormous space of possible solutions effectively. GAs operates on a population of potential solutions applying the principle of survival of the fittest to produce better estimates to a solution. At each generation, a new set of estimates is created by the procedure of selecting individuals according to their level of fitness in the problem domain and breeding them together using operators hired from natural genetics. They generate a classification of populations by using a selection mechanism, crossovers and mutation according to the search mechanism.GA is not reliant to the starting point of the research. It does not want any derivative information of the objective function or the constraint functions. It has a minimum chance of being trapped in a local minimum.

In a GAs, a population of strings (chromosomes), which encode candidate solutions (individuals) to an optimization problem, evolves to better solutions [28]. Each decision which is variable in the parameter set, is encoded as a binary string and these are concatenated to form a chromosome. The use of Gray coding has been advocated as a method of overcoming the hidden representational bias in conventional binary representation as the Hamming distance between adjacent values is constant [29-30].

4.3 Chromosome Representation

The first step in the GA is to generate a primary population. This is usually reached by generating the necessary number of individuals using a random number generator that uniformly distributes numbers in the desired range. Each chromosome in proposed GA is a 1×6 array as being demonstrated in Fig 7, where B_g, A, J_s, k_d, α_p and g are air-gap flux density, electrical loading, current density, diameter ratio, relative magnet width and the air-gap length respectively. Every generation has a chromosome population of 50 and gets randomly selected from the first generation.

B_g	A	J_s	k_d	α_p	g

Fig. 7. Chromosome representation (1 × 6 array)

It should be noted that the presented chromosome contains the genes "K_w" and "N_{ph}". The fitness function depends on all the mentioned genes tacitly as the ratios "K_e", "K_i", "K_p", and parameters like the outer diameter and the total length of machine are functions of the genes.

Chromosome variables or genes have real values, so real coding is applied for normalizing each gene as shown in Fig. 1b. Linear normalization results from:

$$G_{Normal} = \frac{0.8 - 0.2}{G_{max} - G_{min}}(G - G_{min}) \qquad (45)$$

where "G" is the chromosome gene value varies between "G_{min}" and "G_{max}". The normalized values are limited between upper and lower limits 0.8 and 0.2, respectively.

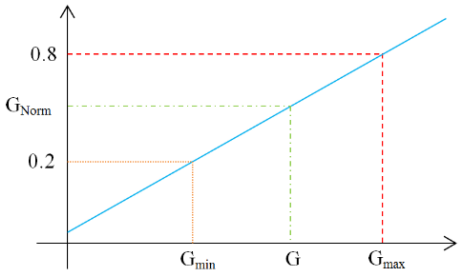

Fig. 8. Real-gene coding (linear normalization)

4.4 Crossover

The basic operation for producing new chromosomes in the GA is the Crossover. Like its counterpart in nature, crossover produces new individuals that have some parts of both parent's genetic material. The simplest form of the crossover is the single-point crossover, described in the Overview of GAs. In this section, a number of variations on crossover are described and debated and the relative merits of each have been reviewed [30].

The elitist method is used as a selection operator for two-point crossover as being shown in Fig 9. At first, two random numbers between one and "chromosome length – 1" are generated (1 ≤ random number ≤ chromosome length – 1).

4.5 Mutation

In natural evolution, mutation is a random procedure that one allele of a gene is replaced by another to produce a new genetic structure. In GAs, mutation is randomly applied with low probability. In this paper the range 0.005 and 0.05 is selected and it modifies the elements in the chromosomes. Usually considered as a background operator, the role of mutation is often seen as providing certitude that the probability of searching any given string will be never zero, also acting as a safety net to recover good genetic material that may be lost through the action of selection and crossover [28-29]. With non-binary representations, mutation is achieved by either perturbing the gene values or random selection of new values within the allowed range.

In GA programming, selecting fitness function to attain the best solution of a problem is very important [31]. An unsuitable fitness function may lead to the wrong answer. Another possible problem may happen when the created genes are quite better than other genes [33], and the answer may lead to a local solution. In this paper, the AFPM machine efficiency (eq. 38) is selected as the fitness function is calculated for each step and chromosome.

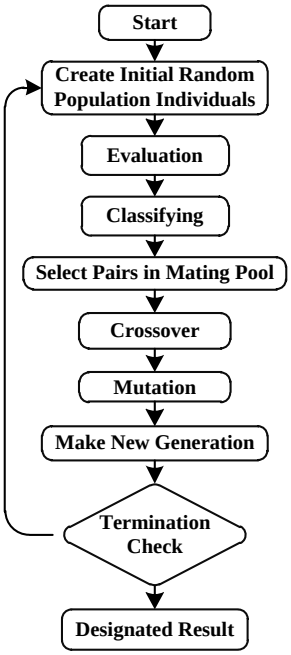

Fig. 9. Genetic Algorithm Flowchart

In Fig 9. Genetic algorithm flowchart and in Fig 10 optimized design flowchart of AFPM machines are illustrated.

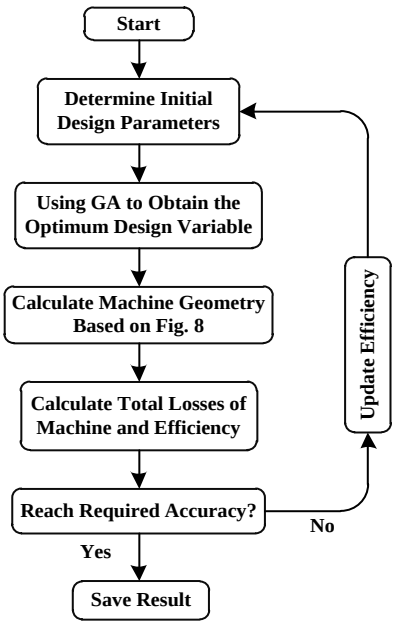

Fig. 10. Design Optimization of AFPM Machine Flowchart

5. Sensitivity Analysis of AFPM Machine

In This paper, sensitivity analysis is used in order to achieve more design ascendancy and realize machine`s behavior on design criteria in AFPM machine. The results of the sensitivity analysis in the selections are used to define lower bound and upper bound of the design variations in genetic algorithm.

One of the most important design parameters of AFPM machines is "k_d" diameter ratio that selecting appropriate value for this parameter has high influence in machine`s performance. In Fig. 11 the efficiency of the machine is shown by using different values of diameter ratio. According to Fig 11, by increasing the k_d, the efficiency of the machine will be decreased. Also the required number of winding turns will be increased so that radial length of the end winding will increase too. This issue is due to the increased copper losses that is the dominated loss of the machine in low-speed application.

In addition, according to Fig 12, increasing k_d is because of the stator`s outer diameter increment and consequently total volume of the machine and core losses.

Air-gap flux density is one of the main design parameter that has influence on the machine`s efficiency. In Fig. 13 the efficiency of the machine is plotted for different values of air-gap flux density. According to Fig 13, by increasing B_g, the efficiency of machine will be increased. Also, air-gap flux density should be selected according to the stator teeth and the stator material saturation. High value of flux density could be reached by using high-quality material, that this issue made machines cost extremely high.

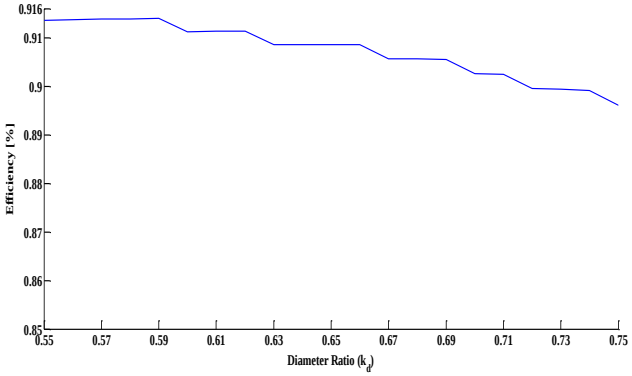

Fig. 11. Sensitivity analysis of machine efficiency versus diameter ratio (k_d)

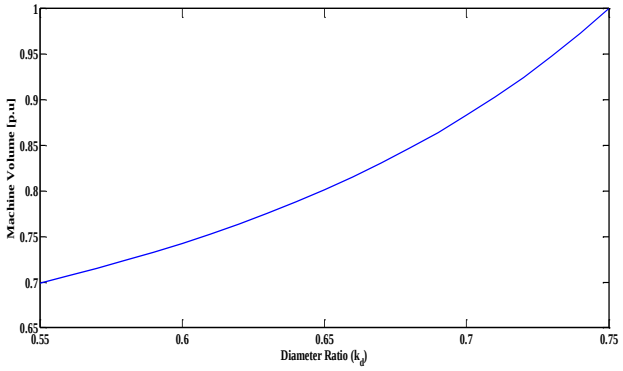

Fig. 12. Sensitivity analysis of machine volume versus diameter ratio (k_d)

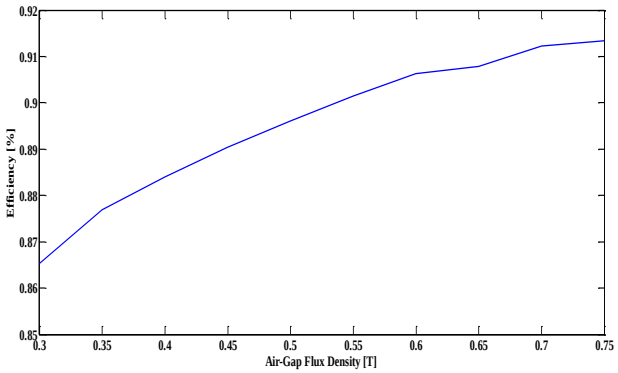

Fig. 13. Sensitivity analysis of machine volume versus air-gap flux density

Current density is one of the design parameters that affects operations and the thermal behavior of the machines. By increasing the current density, the cross section of conductor will be decreased (Eq. 26) and the phase resistance will increase. As a result, the machine`s efficiency will be decreased. On the other hand, by increasing the current density, the machine`s volume will be reduced. Also, this issue will be caused because of reducing coppers that are used in machine and consequently machine cost. The effects of current density on machine`s efficiency and machine`s volume are shown in Fig 14 and Fig 15 respectively.

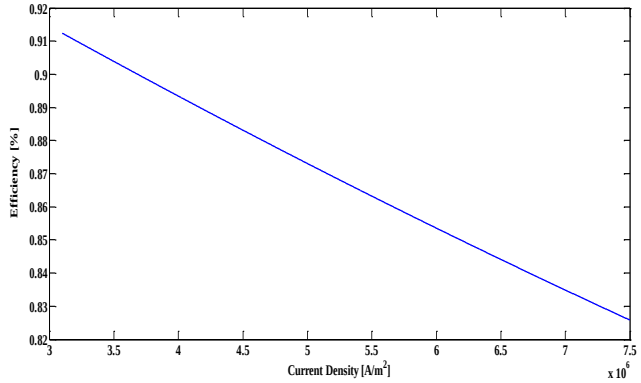

Fig. 14. Sensitivity analysis of machine efficiency versus current density

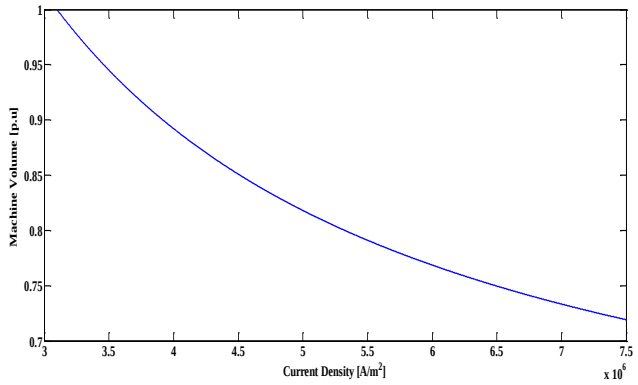

Fig. 15. Sensitivity analysis of machine volume versus current density

6. Result of optimization

The optimization is executed for fitness function (minimizing total loss). Variations for every generation are shown in Fig. 16. According to fitness function, the goal is to minimize the total loss of the machine. We set weight 0.9 and 0.1 for both copper loss and core loss respectively hence copper loss is the dominant loss in low peed machines.

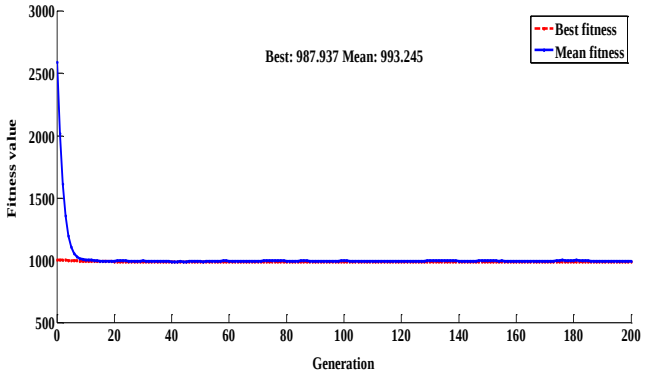

Fig. 16. Fitness Function versus chromosomes in each generation

The design data of double stage inner rotor slotted AFPM machine for both initial and optimized design are presented in table 2.

Table 2. Design data for initial design and optimized design using GA

Design Data	Initial	GA
k_d	0.6	0.553
B_g	0.6	0.75
A	30000 A/m	31751.1A/m
J_s	3.1×10^6 A/m^2	3.108×10^6 A/m^2
g	2mm	2mm
α_p	0.700	0.681
D_{out}	393.2mm	355.3mm
D_{in}	235.9mm	196.5mm
L_{rotor}	17.8mm	19.5mm
L_{ys}	13.7mm	15mm
L_{PM}	3.1mm	5.5mm
L_{slot}	29.1mm	33.1mm
P_{Cu}	1048.5 W	863.6 W
P_{Core}	119.5 W	124.06W
Efficiency	90.4%	91.76%

The minimum loss of the machine is obtained when genetic algorithm is 987.66 watt and the initial designed loss was 1168 watt. The value of total losses (copper losses and core losses) is shown separately in Fig. 17. Also, the maximum efficiency of the machine for initial design and optimized design are shown in Fig 18.

According to Fig. 19, the volume of optimized machine is reduced and consequently, the machine`s weight will decrease. This issue can be seen in Fig. 20.

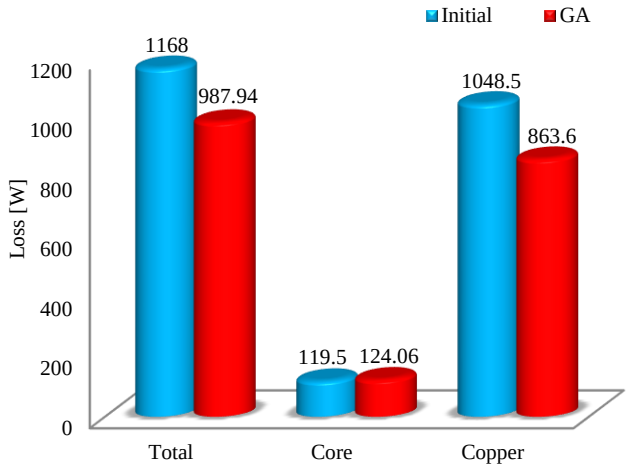

Fig. 17. Value of losses for initial design and optimized design using GA

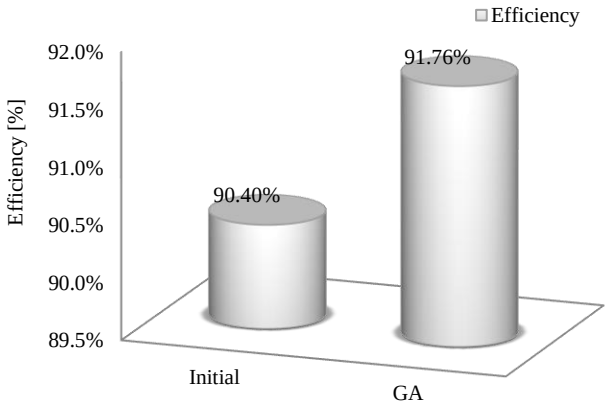

Fig. 18. Efficiency of design AFPM machine

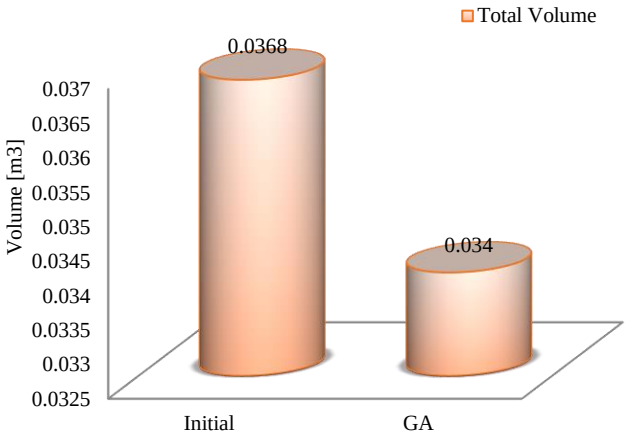

Fig. 19. Volume of machine for initial design and optimized design using GA

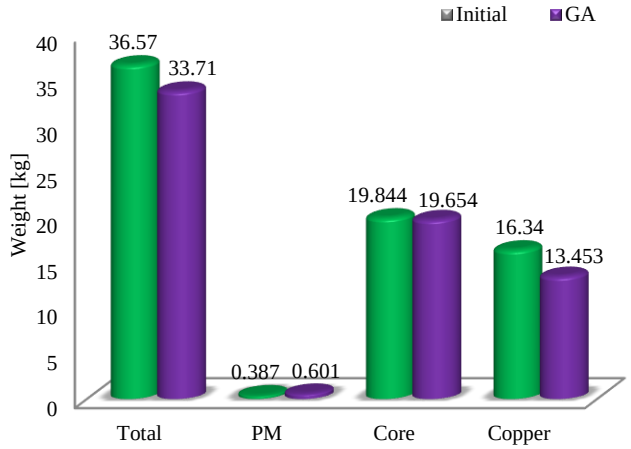

Fig. 20. Weight of machine for initial design and optimized design using GA

7. Finite Element Analysis

In many literates, it has been reported that an axial flux machine has an intrinsic 3D geometry. Therefore, analytical or 2D finite element analysis does not yield adequate accuracy in computations because it is usually performed on the average radius [33-35]. Although, 3D finite element method is time consuming, it is considered to use it to analyze AFPM machines behaviors and allow an accurate analysis of magnetic devices considering geometric details and magnetic nonlinearity. So, it is a suitable technique for analyzing AFPM machines.

In this paper, the result of 3D finite element analysis is presented. The software package, CEDRAT FLUX 3D has been used to execute all simulations. The model of studied AFPM machine is illustrated in Fig 21. Mesh diagram of the studied machine is shown in Fig 22. The density of meshes in stator teeth and PMs are increased because of an accurate simulation. In Fig 23 the flux diagram of the studied machine is shown. It shows that maximum flux density in hotspots is 2.158 T.

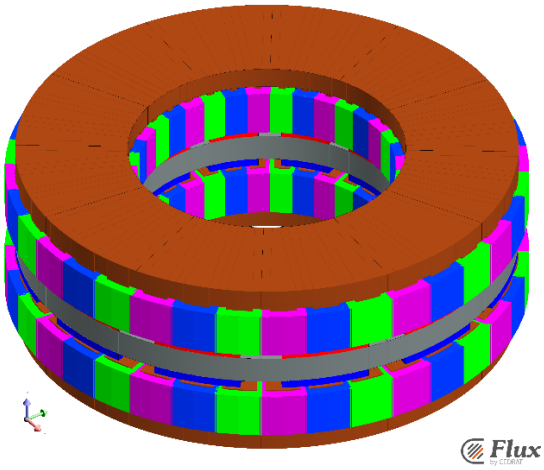

Fig. 21. Studied AFPM machine model

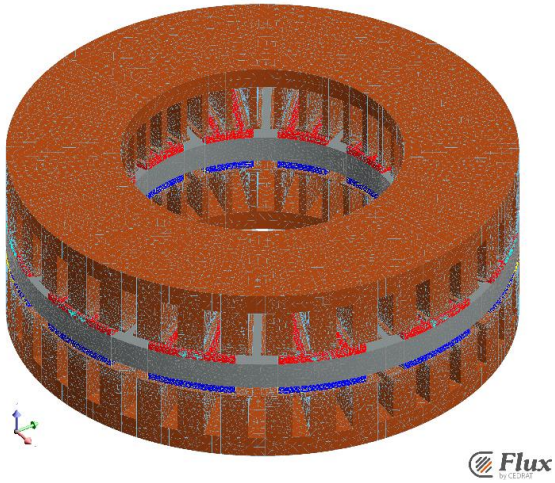

Fig. 22. Studied AFPM machine mesh model

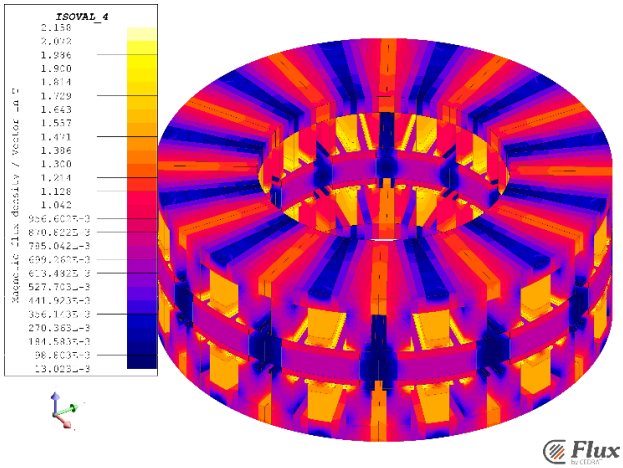

Fig. 23. Flux density distribution in the Studied AFPM machine

One of the most main characteristics of the machine is the air-gap flux density. In Fig 24 air-gap flux density caused by permanent-magnets placed in the middle of air-gap plane is shown.

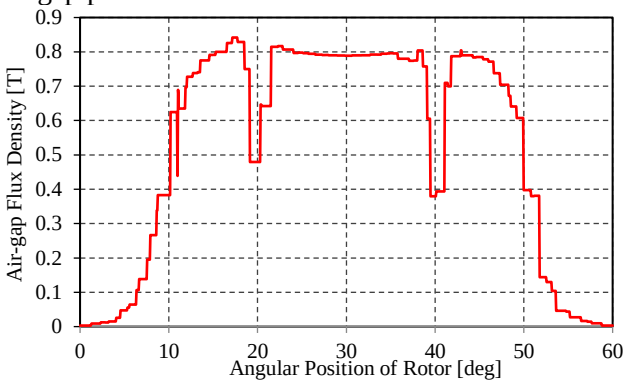

Fig. 24. Air-gap flux density in average radius calculated by FEM

In Fig 25, the induced phase voltages are shown. Moreover, the evaluation between the analytical method and the time transient three dimensional finite element analysis is given in table 3. According to the obtained results in table 3, it is obvious that there is an acceptable agreement between the design necessities and the finite element analysis.

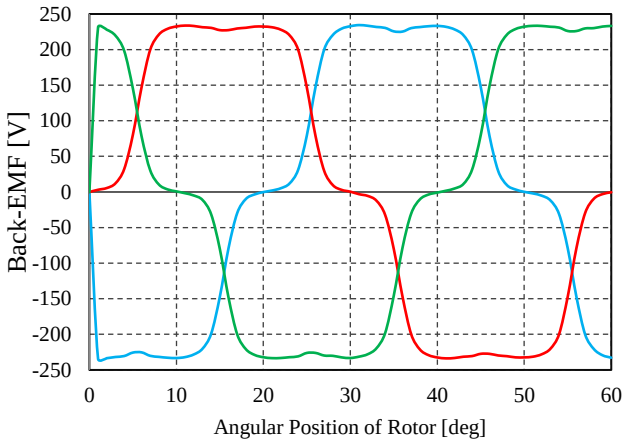

Fig. 25. Induced phase voltages of the machine calculated by FEM

Table 3. FEM results of the machine

Parameter	Analytical	FEM
Maximum Air-gap Flux Density	0.75	0.8
Maximum Flux Density in Stator Teeth	1.84	1.81
Maximum Flux Density in Stator	1.4	1.34

Maximum Flux Density in Rotor Disk	1.4	1.32
Induced phase voltage	231	232.8

8. Sensitivity Analysis of Slot opening

The slot opening must be selected properly according to the flux leakage and cogging torque. It is suggested to use finite element sensitivity analysis. The effect of slot opening on air-gap flux density, induced voltage and cogging torque is presented in Fig 26, Fig 27 and Fig 28 respectively.

Slot opening affects the magnetic field in the air-gap. Slot opening reduces the average magnetic flux per pole and also it influences the air-gap flux distribution. As it is shown in Fig. 26, when the slot opening has high value, reluctance of top part of the slot is remarkable and it leads to the reduction of the flux density under the slot opening area. The air-gap flux density at the edge of the stator teeth under slot opening has a sharp peak. This is known as the slot edge effect [36].

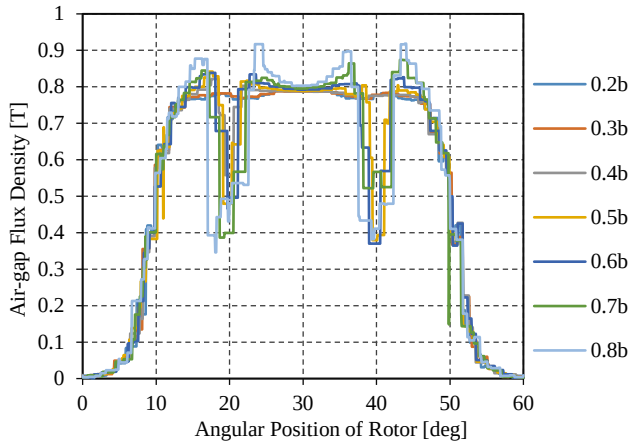

Fig. 26. Effect of different slot opening on air-gap flux density calculated by FEM

According to Fig. 27a and Fig. 27b, back-EMF is reduced under the slot opening area. Reducing the back-EMF in top part of waveform is caused by generating harmonic components.

In axial flux PM machines, cogging torque is generated by the interaction between PMs and stator teeth. It is the peripheral component of attractive force that tries to maintain the alignment between the stator teeth and the PMs. Cogging torque is an adverse effect that adds a ripple component to the appropriate constant output torque [37]. Furthermore, this torque ripple leads to generating vibrations and acoustic noises which is deleterious to the machine`s performance [38-39].

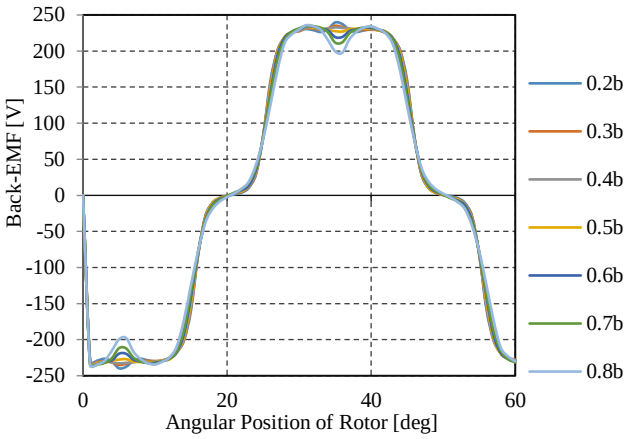

(27a)

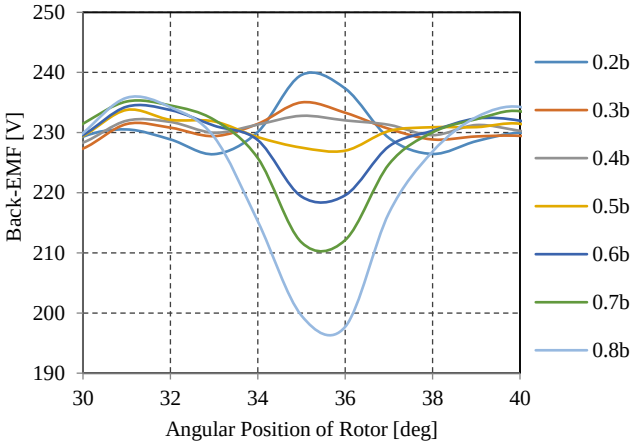

(27b)

Fig. 27. Effect of different slot opening on back-EMF calculated by FEM

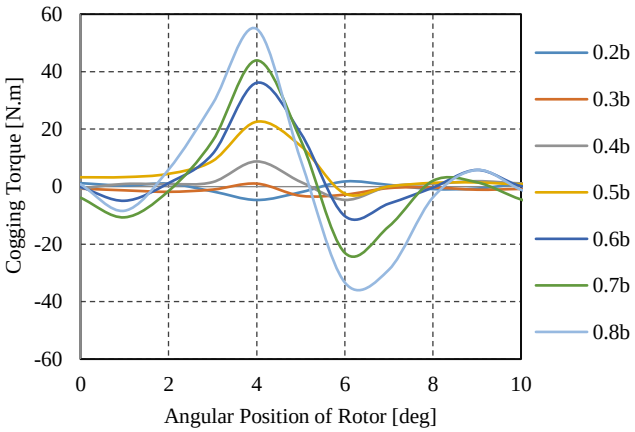

Fig. 28. Effect of different slot opening on cogging torque calculated by FEM

It is obvious that the slot opening has important impact on the cogging torque. In some researches, cogging torque can be effectively reduced by regulating the slot opening [40-42]. In order to find an admissible value of slot opening according to the mechanical constrains, finite element sensitivity analysis is executed for different value of slot opening. It should be mentioned that slot opening is considered as a function of the coil span. In Fig. 28 presents the impact of varying slot opening on cogging torque that is calculated by FEM. As it is demonstrated in Fig. 28, by reducing the slot opening and making the top part of the slot close, cogging torque is decreasing. Consequently, the slot opening should be the minimum acceptable value but the mechanical limitations of the minimum slot opening for inserting coils in the slot must be adhered.

9. Conclusion

Design procedure of AFPM machines were presented completely. The impact of diameter ratio and the current density as two key parameters that have special effect on machine efficiency was studied. Diameter ratio has effects on volume, mass and the efficiency; also it should be selected adequately. Moreover, the current density influences on both volume and efficiency of the machine strictly. Therefore, to obtain high-efficiency, Low value of diameter ratio and current density is considered.

Maximum efficiency of an AFPM machine was explored by using sensitivity analysis and GA with respect of practical and performance limitations. Obtaining lower loss and higher efficiency of the machine is the objective of this optimization.

As a design point, selecting desired value of slot opening is proposed to reduce the harmonic of inducted voltage, cogging torque and consequently the acoustic noises.

References

[1] Waide, P.; Brunner, C. U., "Energy-Efficiency Policy Opportunities for Electric Motor-Driven Systems," International Energy Agency (IEA), 2008.

[2] Boglietti, A.; EL-Refaie, A.M.; Drubel, O.; Omekanda, A.M.; Bianchi, N.; Agamloh, E.B.; Popescu, M.; Di Gerlando, A.; Bartolo, J.B., "Electrical Machine Topologies: Hottest Topics in the Electrical Machine Research Community," Industrial Electronics Magazine, IEEE, vol.8, no.2, pp.18,30, June 2014.

[3] S. Huang; J. Luo; F. Leonardi, A.T. Lipo, "A comparison of power density for axial flux machines based on general purpose sizing equations," IEEE Transactions on Energy Conversion, vol.14, no.2, pp.185,192, Jun 1999.

[4] Surong Huang; JianLuo; Leonardi, F.; Lipo, T.A., "A general approach to sizing and power density equations for comparison of electrical machines," Industry Applications, IEEE Transactions on, vol.34, no.1, pp.92,97, Jan/Feb 1998.

[5] Giulii Capponi, F.; De Donato, G.; Caricchi, F., "Recent Advances in Axial-Flux Permanent-Magnet Machine Technology," IEEE Transactions on Industry Applications, Vol.48, No.6, pp.2190-2205, Nov.-Dec. 2012.

[6] Kahourzade, S.; Mahmoudi, A.; Hew Wooi Ping; Uddin, M.N., "A Comprehensive Review of Axial-Flux Permanent-Magnet Machines," Electrical and Computer Engineering, Canadian Journal of, vol.37, no.1, pp.19,33, winter 2014.

[7] Azzouzi, Jaouad; Barakat, G.; Dakyo, B., "Quasi-3-D analytical modeling of the magnetic field of an axial flux permanent-magnet synchronous machine," Energy Conversion, IEEE Transactions on, vol.20, no.4, pp.746-752, Dec. 2005.

[8] Chan, C.C., "Axial-Field Electrical Machines - Design and Applications," Energy Conversion, IEEE Transactions on, vol.EC-2, no.2, pp.294-300, June 1987.

[9] De Donato, G.; Capponi, F.G.; Rivellini, G.A.; Caricchi, F., "Integral-Slot Versus Fractional-Slot Concentrated-Winding Axial-Flux Permanent-Magnet Machines: Comparative Design, FEA, and Experimental Tests," Industry Applications, IEEE Transactions on, vol.48, no.5, pp.1487-1495, Sept.-Oct. 2012.

[10] Jara, W.; Tapia, J.A.; Bianchi, N.; Pyrhönen, J.; Wallace, R., "Procedure for fast electromagnetic design of axial flux permanent magnet machines," Electrical Machines (ICEM), 2014 International Conference on, vol., no., pp.1396-1402, 2-5 Sept. 2014.

[11] Parviainen, A.; Pyrhonen, J.; Kontkanen, P., "Axial Flux Permanent Magnet Generator with Concentrated Winding for Small Wind Power Applications," Electric Machines and Drives, 2005 IEEE International Conference on, vol., no., pp.1187,1191, 15-15 May 2005.

[12] J. F. Gieras, R. J. Wing, and M. J. Kamper, Axial-flux Permanent Magnet Machines, Dordrecht, Germany: Kluwer, 2004.

[13] M. Sadeghierad, A. Darabi, H. Lesani, H. Monsef, "Optimal design of the generator of microturbine using genetic algorithm and PSO," Electrical Power and Energy Systems, Vol. 32, pp. 804–808, 2010.

[14] J. P. Pyrhonen, T. Jokinen, V. Hrabovcova, Design of Rotating Electrical Machines, John Wiley and Sons, 2014.

[15] Cros, J.; Viarouge, P., "Synthesis of high performance PM motors with concentrated windings," Energy Conversion, IEEE Transactions on, vol.17, no.2, pp.248-253, Jun 2002.

[16] Magnussen, F.; Sadarangani, C., "Winding factors and Joule losses of permanent magnet machines with concentrated windings," Electric Machines and Drives Conference, 2003. IEMDC'03. IEEE International, vol.1, no., pp.333-339 vol.1, 1-4 June 2003.

[17] EL-Refaie, A.M.; Jahns, T.M., "Optimal flux weakening in surface PM machines using fractional-slot concentrated windings," Industry Applications, IEEE Transactions on, vol.41, no.3, pp.790-800, May-June 2005.

[18] Chang-Chou Hwang; Cho, Y.H., "Effects of leakage flux on magnetic fields of interior permanent magnet synchronous motors," Magnetics, IEEE Transactions on, vol.37, no.4, pp.3021-3024, Jul 2001.

[19] Ronghai Qu; Lipo, T.A., "Analysis and modeling of air-gap and zigzag leakage fluxes in a surface-mounted

permanent-magnet Machine," Industry Applications, IEEE Transactions on, vol.40, no.1, pp.121-127, Jan.-Feb. 2004. doi: 10.1109/TIA.2003.821790
[20] H. Jussila, "Concentrated Winding Multiphase Permanent Magnet Machine Design and Electromagnetic Properties – Case Axial Flux Machine," Ph.D. Dissertation, Univ. Technology, Lappeenranta, Finland, 2009.
[21] Mahmoudi, A.; Kahourzade, S.; Rahim, N.A.; Ping, H.W.; Uddin, M.N., "Design and prototyping of an optimized axial-flux permanent-magnet synchronous machine," Electric Power Applications, IET, vol.7, no.5, pp.338-349, May 2013.
[22] A. Parviainen, "Design of axial flux permanent-magnet low-speed machines and performance comparison between radial-flux and axial-flux machines," Ph.D. Dissertation, Univ. Technology, Lappeenranta, Finland, 2005.
[23] Mueller, M.A.; McDonald, A.S.; Macpherson, D.E., "Structural analysis of low-speed axial-flux permanent-magnet machines," Electric Power Applications, IEE Proceedings -, vol.152, no.6, pp.1417-1426, 4 Nov. 2005.
[24] J. F. Gieras, Permanent Magnet Motor Technology: Design and Applications, Third Edition, Dordrecht, Germany: CRC Press, 2009.
[25] D. C. Hanselman, Brushless Permanent-Magnet Motor Design, USA,Magna Physics Publishing, 2003.
[26] El-Hasan, T.S.; Luk, P.C.K.; Bhinder, F.S.; Ebaid, M.S., "Modular design of high-speed permanent-magnet axial-flux generators," Magnetics, IEEE Transactions on, vol.36, no.5, pp.3558-3561, Sep 2000.
[27] R. Dutta, L. Chong, and F. M. Rahman, "Analysis and experimental verification of losses in a concentrated wound interior permanent magnet machine," Progress in Electromagnetics Research B, Vol. 48, 221-248, 2013.
[28] D. E. Goldberg, Genetic Algorithms in Search, Optimization and Machine Learning. Addison Wesley Publishing Company, January 1989.
[29] C. L. Karr, "Design of an Adaptive Fuzzy Logic Controller Using a Genetic Algorithm", Proc. ICGA 4, pp. 450-457, 1991.
[30] A. Chipperfield, P. Fleming, H. Pohlheim, C. Fonseca, "Genetic Algorithm Toolbox for Use with MATLAB," Department of Automatic Control and System Engineering, University of Sheffield.
[31] Rashtchi, V.; Rahimpour, E.; Fotoohabadi, H., "Parameter identification of transformer detailed model based on chaos optimization algorithm," Electric Power Applications, IET, vol.5, no.2, pp.238-246, Feb. 2011.
[32] Acikbas, S.; Soylemez, M.T., "Coasting point optimization for mass rail transit lines using artificial neural networks and genetic algorithms," Electric Power Applications, IET, vol.2, no.3, pp.172-182, May 2008.
[33] F. Marignetti, V. DelliColli, Y.Coia, "Design of Axial Flux PM Synchronous Machines Through 3-D Coupled Electromagnetic Thermal and Fluid-Dynamical Finite-Element Analysis," IEEE Transactions on Industrial Electronics, vol.55, no.10, pp.3591-3601, Oct. 2008.
[34] A. Parviainen, M. Niemela, J. Pyrhonen, "Modeling of axial flux permanent-magnet machines," IEEE Transactions on Industry Applications, vol.40, no.5, pp.1333-1340, Sept.-Oct. 2004.
[35] Upadhyay, P.R.; Rajagopal, K.R., "FE Analysis and Computer-Aided Design of a Sandwiched Axial-Flux Permanent Magnet Brushless DC Motor," Magnetics, IEEE Transactions on, vol.42, no.10, pp.3401-3403, Oct. 2006.
[36] Hung Vu Xuan; Lahaye, D.; Polinder, H.; Ferreira, J.A., "Influence of Stator Slotting on the Performance of Permanent-Magnet Machines with Concentrated Windings," Magnetics, IEEE Transactions on, vol.49, no.2, pp.929,938, Feb. 2013.
[37] Studer, C.; Keyhani, A.; Sebastian, T.; Murthy, S.K., "Study of cogging torque in permanent magnet machines," Industry Applications Conference, 1997. Thirty-Second IAS Annual Meeting, IAS '97., Conference Record of the 1997 IEEE, vol.1, no., pp.42-49 vol.1, 5-9 Oct 1997.
[38] Sang-Moon Hwang; Jae-Boo Eom; Hwang, Geun-Bae; Weui-Bong Jeong; Yoong-Ho Jung, "Cogging torque and acoustic noise reduction in permanent magnet motors by teeth pairing," Magnetics, IEEE Transactions on, vol.36, no.5, pp.3144-3146, Sep 2000.
[39] Sang-Moon Hwang; Jae-Boo Eom; Yoong-Ho Jung; Deug-Woo Lee; Kang, Beom-Soo, "Various design techniques to reduce cogging torque by controlling energy variation in permanent magnet motors," Magnetics, IEEE Transactions on, vol.37, no.4, pp.2806-2809, Jul 2001.
[40] Zhu, Z.Q.; Howe, D., "Analytical prediction of the cogging torque in radial-field permanent magnet brushless motors," Magnetics, IEEE Transactions on, vol.28, no.2, pp.1371-1374, Mar 1992.
[41] Ackermann, B.; Janssen, J.H.H.; Sottek, R.; van Steen, R.I., "New technique for reducing cogging torque in a class of brushless DC motors," in IEE Proceedings B - Electric Power Applications, vol.139, no.4, pp.315,320, Jul 1992.
[42] Gieras, J.F., "Analytical approach to cogging torque calculation of PM brushless motors," Industry Applications, IEEE Transactions on, vol.40, no.5, pp.1310-1316, Sept.-Oct. 2004.